

A High Step-Up DC-DC Converter Using Coupled Inductor With Fuzzy Logic Control

Nancy.R¹, Radhalakshmi.K²

M.E. Power Electronics & Drives, Department of EEE, Sethu Institute of Technology
Kariyapati, India¹

M.E. Power Electronics & Drives, Department of EEE, Sethu Institute of Technology
Kariyapati, India²

ABSTRACT—In this paper, a high step-up converter using coupled inductor with Fuzzy Logic Control is analyzed and simulated. The converter uses a coupled inductor and a switched capacitor circuit to achieve high voltage conversion ratio. Two capacitors and diodes constitute the switched capacitor circuit. The two capacitors are charged in parallel during the switch-off period and are discharged in series during the switch-on period by the energy stored in the coupled inductor to achieve a high step-up voltage gain. Switch voltage stress and the circulating current are reduced by a clamp circuit which is composed of a diode followed by a capacitor. Thus the efficiency of the converter is improved. The operating principle and the steady state analysis are discussed in detail. A Fuzzy logic controller is designed such that it eliminates the Voltage Drift problem.

INDEX TERMS—Coupled Inductor, FLC, Switched Capacitor circuit.

I. INTRODUCTION

Renewable energy sources (RES) have experienced a fast development in recent years. These systems employ with micro sources like PV, fuel cells etc. Though PV cells can be made into array and connected in series to produce high voltage there exist serious problems like shadowing effects, short circuit which drastically reduces its efficiency. In order to overcome such adverse effects this micro source energy is utilized by the high step up converter to produce high voltage and satisfy the demands. Conventional boost converters can't provide such a high DC voltage gain for extreme duty cycle.

Thus high step up dc-dc converters are used as front

end converters to step from low voltage to high voltage which are required to have a large conversion ratio, high efficiency and small volume [1]. In some converters active clamp circuit is used to overcome voltage spikes caused by the leakage inductance of the coupled inductor. Though ZVS technique is employed for soft switching it can't sustain light loads [2]. Different switching structures are formed either two capacitor or two inductor with two-three diodes. Both the step up and step down operations can be performed in this topology. Performance of hybrid converters are better than classical converters but still its costlier to implement [3]. Low level voltage from the PV, fuel cells is connected to Kilo watt level using step up dc-dc converter and inverter circuits. Voltage spikes and switching losses are eliminated by active clamping. In dc-ac, inverter always tends to draw ac ripple current at twice the output frequency. Resonant inductors cost and circuit volume is high [4]. In some converters high voltage conversion is obtained by changing transformer turns ratio which will increase the overall efficiency but still the operation of main switch involves hard switching and also EMI noise gets raised [5]. Impacts of SiC (silicon carbide) MOSFETS on converter, switching and conduction losses are reduced even though fast switching is done. Si diodes have ideal, but still SiC devices processes large amount of ringing current at turn OFF relatively to other devices. Package of external diode and the diode itself have more parasitic capacitances that are added to the devices parasitic aggravating the ringing [6]. Here, the voltage step is done without a transformer and a high voltage gain is achieved without an extremely high duty ratio but still the circuit becomes more bulky as more number of passive components are used [7]. Though this converter provides

a non-pulsating current by using an auto transformer, duty ratio is limited by 0.5 and not suitable for non-linear loads [8]. Here voltage stress of the active switch is reduced thereby the conversion efficiency is improved. This converter requires a multi winding transformer which makes the circuit design complex [9]. This converter avoids extremely narrow turn off period, ripples and switching losses are eliminated by ZVS technique. It uses two coupled inductors which makes the circuit complex [10]. In this converter no additional magnetic components used, switching losses are minimized by adopting a regenerative snubber circuit. As the circuit uses more switches controlling is complex [11]. In this converter high voltage gain is obtained but the circuit has more passive components [12]. It employees single ended scheme cost is reduced. Galvanic isolation is needed, but suitable only for low power and frequency applications [13], [14]. In this converter no need of extreme duty ratio but if conduction losses or switching losses occurs the efficiency is reduced [15]. It is possible to generate the non-isolated dc-dc converters but the major drawback is that switching frequency must be maintained constant and the turn ratio of the auto transformer must be unity [16]. Some converters operate at very high frequency with fast transient response. The main switch is fabricated from an integrated power process, the layouts can be changed to vary the parasitic, however design of switch layout is complex, fixed frequency and constant duty ratio must be maintained [17]. This converter provides high voltage gain and can be employed for high power applications however the duty ratio is limited to 0.85 [18], [19]. In this, the energy of the leakage inductor is recycled to the output load directly, limiting the voltage spike on the main switch. To achieve a high step-up gain, it has been proposed that the secondary side of the coupled inductor can be used as flyback and forward converters [20], [21]. In some converters voltage gain is improved through output voltage stacking [22].

II. OPERATING PRINCIPLE OF THE PROPOSED CONVERTER

Fig. 2 shows the circuit configuration of the proposed converter, which consists of a boost converter, coupled inductor, switched capacitor circuit and a clamp circuit. The equivalent circuit of the coupled inductor has a magnetizing inductor L_m , leakage inductor L_k , and an ideal transformer. N_s and N_p is the primary and secondary winding of the ideal transformer, V_{in} DC input voltage, V_o is the DC output voltage, and S main switch.

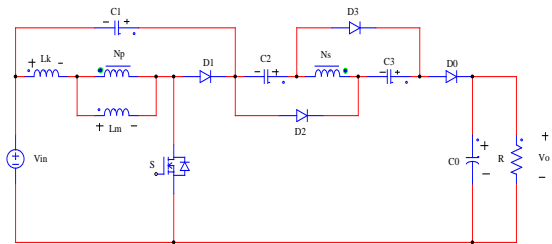


Fig.2 Proposed Converter.

The diodes D_2 , D_3 and capacitors C_2 , C_3 forms the switched capacitor circuit. D_1 , C_1 are the clamp diode and clamp capacitor respectively. The operating principle is that when the switch S is ON, the input supply voltage charges the magnetizing inductor L_m which is in the primary side of the coupled inductor N_p . This N_p induces emf to the secondary side of the coupled inductor which makes the capacitors C_1 , C_2 , C_3 to discharge in series and delivers to the load resistance. The output capacitor C_0 is in charging state. When the switch S is turned OFF, the energy stored in the magnetizing inductor gets discharged and makes the capacitors C_2 , C_3 to charge in parallel. Meanwhile, the D_1 is turned ON and charges the clamp capacitor C_1 , thus reduces the switch voltage stress and the circulating current. The energy stored in C_0 is delivered to the load resistance. Fig. 3 shows the typical waveforms.

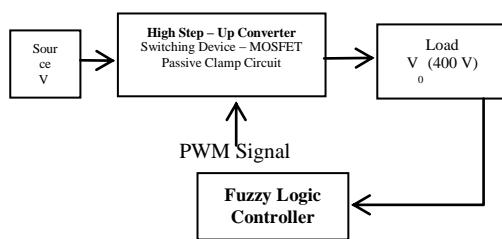


Fig. 1 Block Diagram.

The main objective is to improve the Voltage Gain of the Step-up Converter and also to reduce Voltage stress of the circuit. Further the Voltage Drift problem is reduced using closed loop control of the proposed converter with fuzzy logic controller. From Fig.1, The output voltage from the converter is fed as feed back to the FLC; there it compares the feedback voltage signal and the reference voltage signal to produce PWM pulse which triggers the main switch of the converter.

A High Step-Up DC-DC Converter using Coupled Inductor with Fuzzy Logic Control

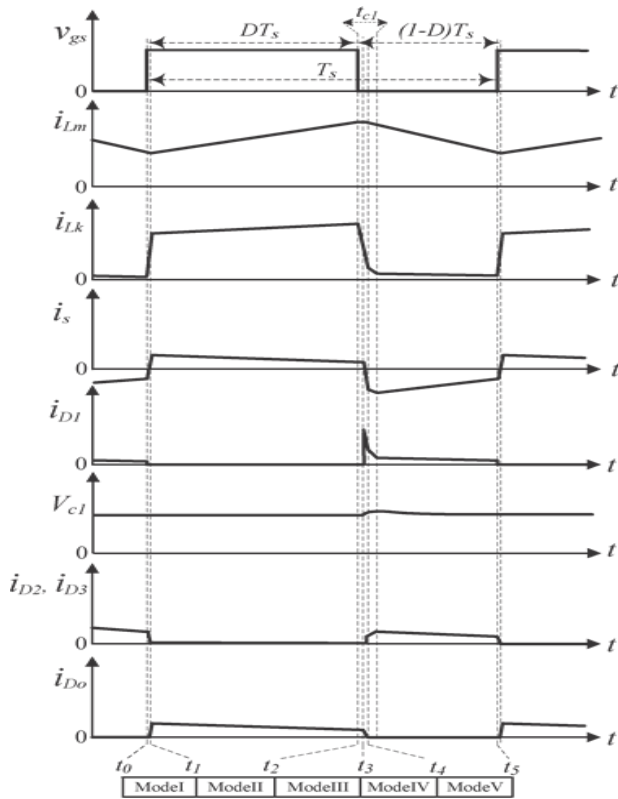


Fig.3 Waveforms of the Proposed converter.

Assumptions to simplify the circuit analysis,

1. Capacitors C_1 , C_2 , C_3 and C_0 are large enough. And so, V_{C1} , V_{C2} , V_{C3} and V_{C0} are considered as constants in one switching period.
2. The power devices are ideal.
3. The coupling coefficient of the coupled inductor k is equal to $L_m / (L_m + L_k)$, and the turn ratio of the coupled inductor n is equal to N_s / N_p .

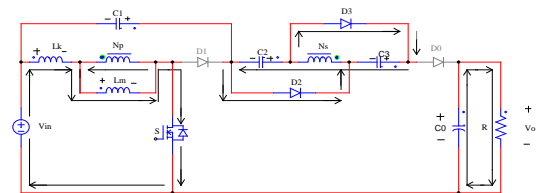
A. Mode of Operation

There are five operating modes in one switching period. Fig. 4 shows the current-flow path of each mode of the circuit.

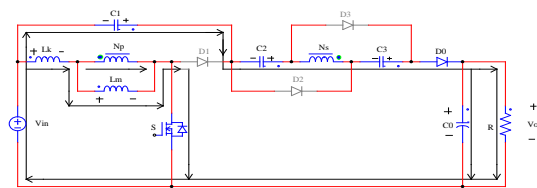
- a) Mode I [t_0, t_1]: In this mode, S is turned on. Diodes D_1 and D_0 are turned off, and D_2 and D_3 are turned on. The current-flow path is shown in fig. 4(a). The leakage inductor L_k charged by V_{in} . Output capacitor C_0 provides its energy to load R . When current i_{D2} becomes zero at $t = t_1$, this operating mode ends.
- b) Mode II [t_1, t_2]: In this mode, S remains turned on. Diode D_1 , D_2 , and D_3 are turned off and D_0 is turned on. The current-flow path is shown in fig. 4(b). Magnetizing inductor L_m charges by V_{in} . The induced voltage V_{L2} on the secondary side of the coupled inductor makes V_{in} , V_{C1} , V_{C2} and V_{C3} , which are connected in series, discharge to high-voltage

output capacitor C_0 and load R . when switch S is turned off this mode ends.

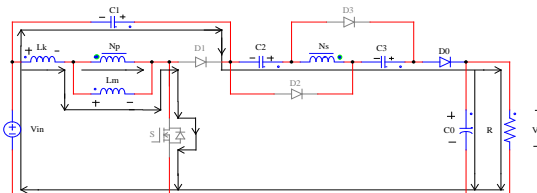
- c) Mode III [t_2, t_3]: In this mode, S is turned off. Diodes D_1 , D_2 , and D_3 are turned off and D_0 is turned on. The current-flow path is shown in fig. 4(c). The energies of L_k and L_m charge the parasitic capacitor C_{ds} of main switch S . Output capacitor C_0 provides its energy to load R . At $t = t_3$, diode D_1 conducts, and this mode ends.
- d) Mode IV [t_3, t_4]: In this mode, S is turned off. Diodes D_1 and D_0 are turned on, and D_2 and D_3 are turned off. The current-flow path is shown in fig. 4(d). The energies of L_k and L_m charge C_1 . The energy of L_k is recycled. Secondary-side voltage V_{L2} of the coupled inductor continues charging high-voltage output capacitor C_0 and load R in series until the secondary current of the coupled inductor is equal to zero. At $t = t_4$, this mode ends.
- e) Mode V [t_4, t_5]: In this mode, S is turned off. Diode D_1 , D_2 , and D_3 are turned on and D_0 is turned off. The current-flow path is shown in fig. 4(e). C_0 is discharged to load R . The energies of L_k and L_m charge the C_1 . L_m is released via the secondary side of the coupled inductor and charges capacitors C_2 and C_3 . Thus, C_2 and C_3 are charged in parallel and L_k charges capacitor C_1 . This mode ends at $t = t_5$.



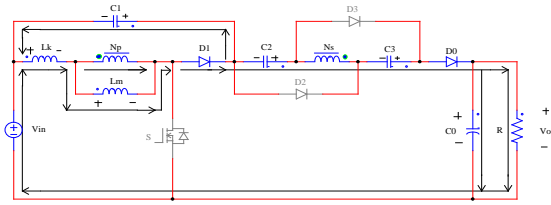
a) Mode I [t_0, t_1].



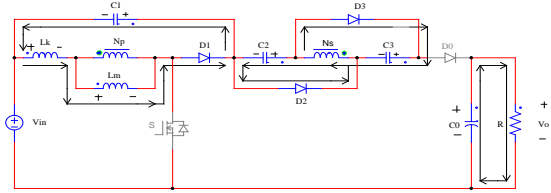
b) Mode II [t_1, t_2].



c) Mode III [t_2, t_3].



d) Mode IV [t₃, t₄].



e) Mode V [t₄, t₅].
Fig. 4 Operating Modes.

III. ANALYSIS OF THE PROPOSED CONVERTER

According to [1], the energy stored in the leakage inductor L_k of the coupled inductor is released to capacitor C_1 . The energy-released duty cycle D_{C1} can be expressed as

$$D_{C1} = \frac{t_{c1}}{T_s} = \frac{2(1-D)}{n+1} \quad (1)$$

The equivalent circuit and state definition of the newly designed converter is depicted in fig.2, where the transformer is modeled as an ideal transformer.

The turn ratio of this ideal transformer is defined as

$$n = \frac{N_2}{N_1} \quad (2)$$

From fig. 4.b),

$$V_{L1}^{ON} = \frac{L_m}{L_m + L_{k1}} V_{in} = KV_{in} \quad (3)$$

$$V_{L2}^{ON} = nV_{L1}^{ON} = nKV_{in} \quad (4)$$

$$V_0 = V_{in} + V_{C1} + V_{C2} + V_{L2}^{ON} + V_{C3} \quad (5)$$

By Voltage Second Balance principle,

$$\int_0^{DT_s} V_{L1}^{ON} dt + \int_{DT_s}^{T_s} V_{L1}^{OFF} dt = 0 \quad (6)$$

$$\int_0^{DT_s} V_{L2}^{ON} dt + \int_{DT_s}^{T_s} V_{L2}^{OFF} dt = 0 \quad (7)$$

By solving (6), (7), we get,

$$V_{L1}^{OFF} = \frac{-Dk}{1-D} V_{in} \quad (8)$$

$$V_{L2}^{OFF} = \frac{-nDk}{1-D} V_{in} \quad (9)$$

As the capacitors are charged during switch OFF mode, the voltage across the capacitors can be obtained from fig.4(e),

$$V_{C1} = \frac{D}{1-D} \cdot V_{in} \cdot \frac{(1+k)+(1-k)}{2} \quad (10)$$

$$V_{C2} = V_{C3} = -V_{L2}^{ON} = \frac{nDk}{1-D} V_{in} \quad (11)$$

Substituting (4), (10), (11) in (5), we get,

$$V_0 = \frac{1+nk}{1-D} \cdot V_{in} + \frac{D}{1-D} \cdot \frac{(k-1)+n(1+k)}{2} \cdot V_{in} \quad (12)$$

$$\frac{V_0}{V_{in}} = \frac{1+nk}{1-D} + \frac{D}{1-D} \cdot \frac{(k-1)+n(1+k)}{2} \quad (13)$$

According to the description of operating modes, voltage stresses on active switch S and diodes D_1 , D_2 , D_3 , and D_0 are given as

$$V_{ds} = \frac{1}{1-D} V_{in} = \frac{V_0 + nV_{in}}{2n+1} \quad (14)$$

$$V_{D1} = \frac{1}{1-D} V_{in} = \frac{V_0 + nV_{in}}{2n+1} \quad (15)$$

$$V_{D2} = V_{D3} = V_{D0} = \frac{n}{1-D} V_{in} = \frac{n(V_0 + nV_{in})}{2n+1} \quad (16)$$

Equations (14)–(16) mean that, under the same voltage ratio, the voltage stresses can be adjusted by the turn ratio of the coupled inductor.

IV. DESIGNING OF PARAMETERS

Let:

- Input Voltage $V_{in} = 24$ V
- Output Power $P_0 = 200$ W
- Switching Frequency $f = 50$ KHz
- Load Resistance $R = 800\Omega$

A. Design Of Coupled Inductor

$$k = \frac{L_m}{L_m + L_k} \quad (17)$$

$$\Delta I_1 = \frac{DkV_{in}}{L_1 f(2D-1)} \quad (18)$$

$$\Delta I_2 = \frac{nDkV_{in}}{L_2 f(2D-1)} \quad (19)$$

From equations (13), (17), (18) & (19) the values of $L_1 = 1.48$ mH, $L_2 = 5.62$ mH are obtained. Here the L_m & L_k values are chosen as 48μ H & 0.25μ H.

B. Selection of Switching Device

IV. POWER MOSFET:

It is chosen as switch as it is cost effective, high commutation speed, low on state resistance, improved gate and high speed power switching.

To verify the performance of the proposed converter, circuit is simulated using MATLAB software. The Converter specifications are as follows:

- 1) Input dc voltage $V_{in} = 24$ V
- 2) Output dc voltage $V_0 = 400$ V
- 3) Maximum output power $P_0 = 200$ W
- 4) Switching frequency $f = 50$ kHz
- 5) Capacitors $C_1 = 56 \mu\text{F}$
 $C_2/C_3 = 22 \mu\text{F}$
 $C_0 = 180 \mu\text{F}$
- 6) Coupled inductor $n = N_p:N_s = 1: 4$
 $L_m \& L_k = 48 \mu\text{H} \& 0.25 \mu\text{H}$

V. FUZZY LOGIC CONTROLLER DESIGN

The block diagram of fuzzy logic controller (FLC) is shown in fig.5. It consists of three main blocks: fuzzification, inference engine and defuzzification. The two FLC input variables are the error E and change in error E*. Depending on membership functions and the rules FLC operates.

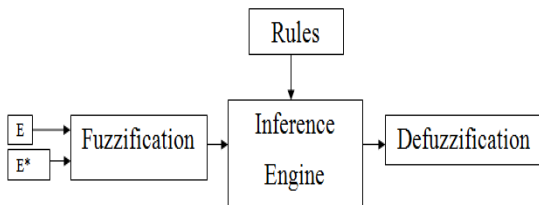


Fig.5 Block Diagram of FLC.

A. Fuzzification

The membership function values are assigned to the linguistic variables using seventeen fuzzy subsets. Table-I shows the rules of FLC. E and E* are input variables, where E is the error between the reference and actual voltage of the system, E* is the change in error in the sampling interval.

B. Inference Engine

Mamdani method is used with Max-Min operation fuzzy combination. Fuzzy inference is based on fuzzy rules. Rules are framed in inference engine block. The output membership function of each rule is given by MIN (Minimum) operator and MAX (Maximum) operator.

C. Defuzzification

The output of fuzzy controller is a fuzzy subset. As the actual system requires a non fuzzy value of Control, defuzzification is required. Defuzzifier is used to convert the linguistic fuzzy sets back into actual value. The membership functions of error (E), change in error (E*) and Duty ratio (D) are shown in fig. 6, 7, 8. Fig.9 shows the representation of the typical Rule Surface of fuzzy logic controller.

TABLE-I
RULE TABLE FOR FLC

E \ E*	N	Z	P
N8	N7	N8	N6
N7	N6	N7	N8
N6	N5	N6	N7
N5	N4	N5	N6
N4	N3	N4	N5
N3	N2	N3	N4
N2	N8	N2	N3
N1	N8	Z	P2
Z	P1	Z	N1
P1	P2	P1	Z
P2	P3	P2	P1
P3	P4	P3	P1
P4	P3	P4	P3
P5	P6	P5	P5
P6	P7	P6	P5
P7	P8	P7	P6
P8	P8	P8	P7

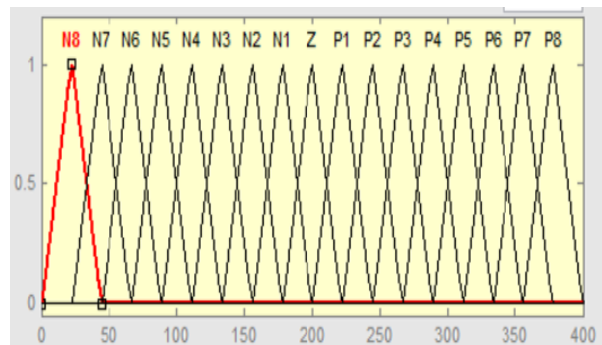


Fig.6 Membership Functions of Error (E).

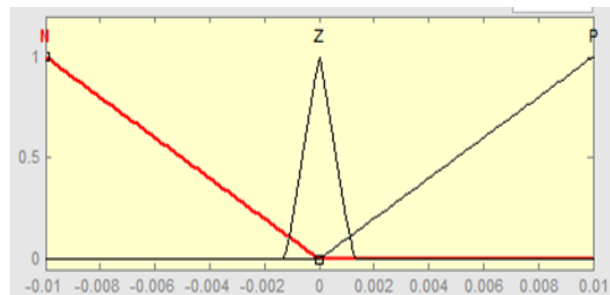


Fig.7 Membership Functions of Change in Error (E*).

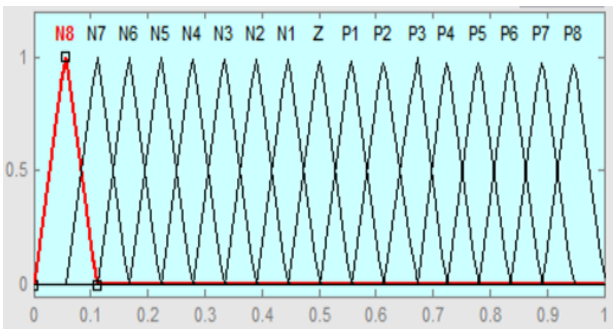


Fig.8 Membership Functions of Duty Ratio (D).

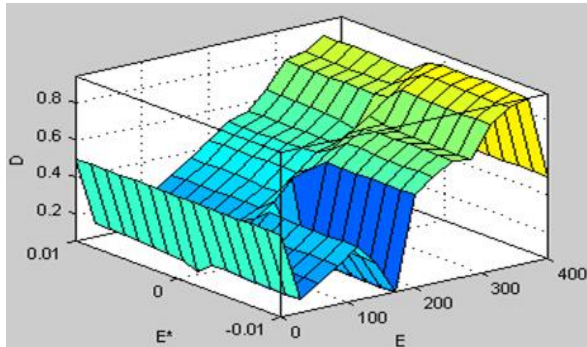


Fig.9 Surface View of Rules of FLC.

VI.SIMULATION DIAGRAMS

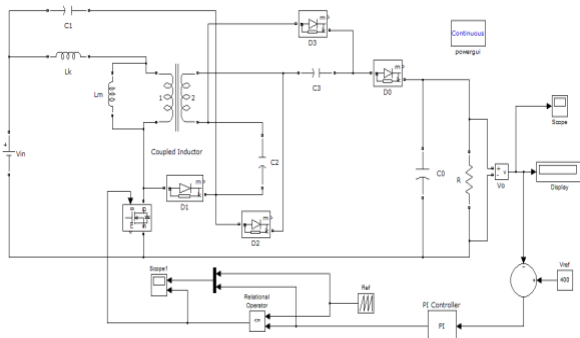


Fig.10 Proposed Converter with PI controller.

Fig.10 shows, A24 V input voltage is fed to the converter, an output voltage of 398.3 V is obtained which is fed back as a feedback voltage to the PI controller; there it compares the feedback and the reference signal from which PWM pulse is generated which triggers the main switch of the converter.

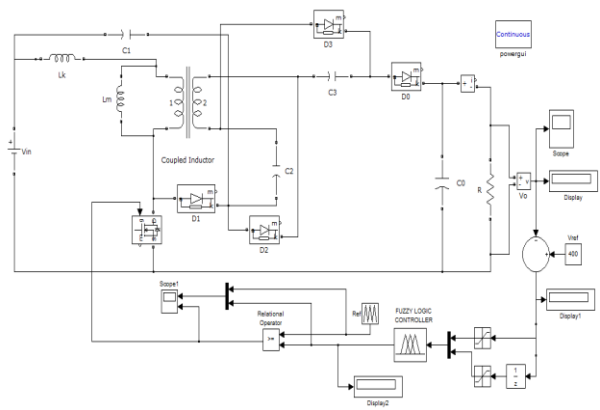


Fig.11 Proposed Converter with FLC.

In fig.11, for the same input voltage the converter is controlled by the newly designed FLC now 399.4 V output voltage is obtained.

VII.SIMULATION RESULTS

A. Simulation Results of Proposed converter with PI controller

Fig. 12 shows the response of the converter with PI controller.

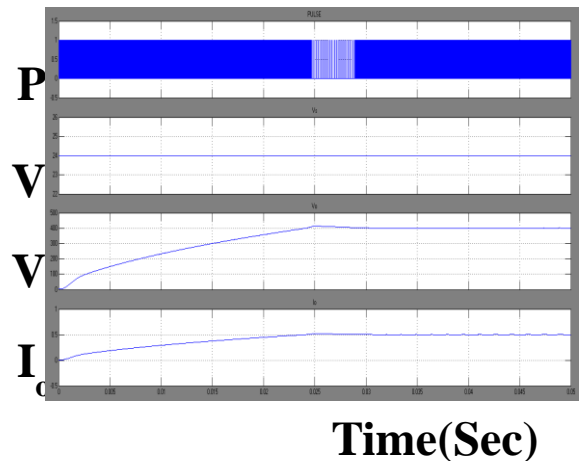


Fig.12 Pulse, Input Voltage, Output Voltage & Output Current ($V_{in} = 24 \text{ V}$, $V_o = 398.3 \text{ V}$ & $I_o = 0.5 \text{ A}$).

The switch voltage stress of the converter with PI controller is shown in fig. 13.

A High Step-Up DC-DC Converter using Coupled Inductor with Fuzzy Logic Control

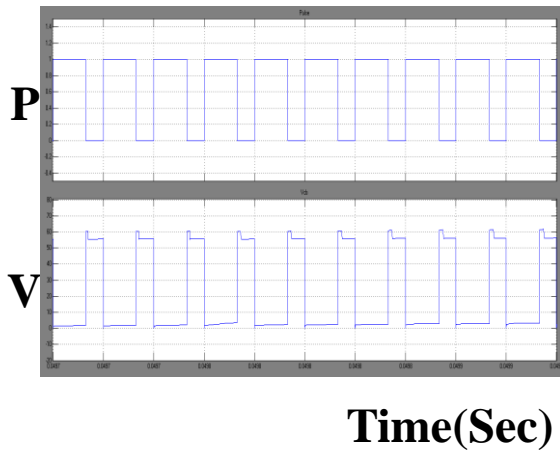


Fig.13 Pulse, Voltage across Switch ($V_{ds}= 55 - 60$ V).

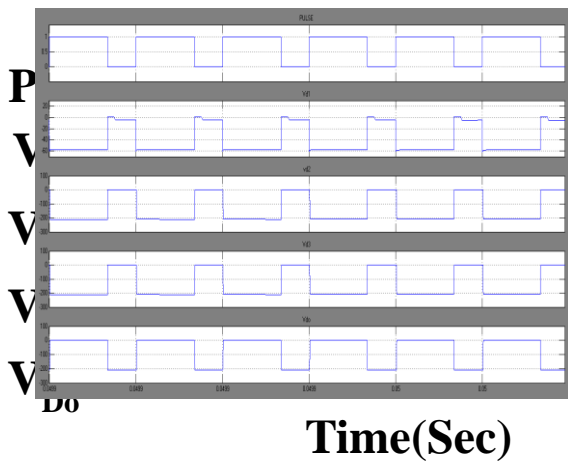


Fig.14 Pulse, Voltage across Diodes($V_{D1}=60$ V, $V_{D2}=V_{D3}=V_{D0}=200$ V).

B. Simulation Results of Proposed Converter with FLC

From fig 15, it is clear that for the designed parameters, required output voltage and current is obtained. The duty ratio of the switch is adjusted by FLC to obtain the required output and also the voltage drift problem is eliminated.

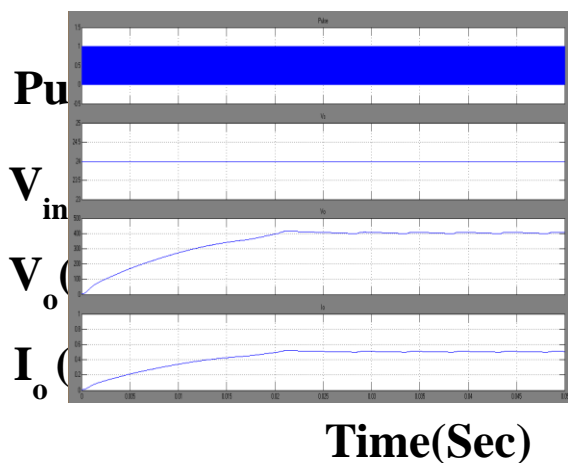


Fig.15 Pulse, Input Voltage Output Voltage & Output Current ($V_{in} = 24$ V, $V_o = 399.4$ V & $I_o = 0.5$ A).

Further from fig 16, the voltage stress of switch is much reduced than the circuit with PI controller.

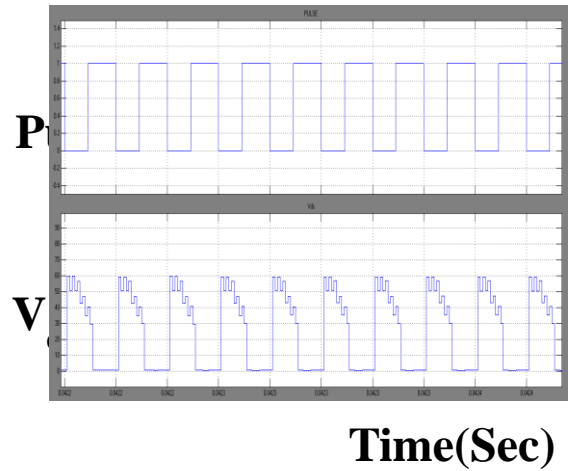


Fig.16 Pulse, Voltage across Switch ($V_{ds}= 30 - 57$ V).

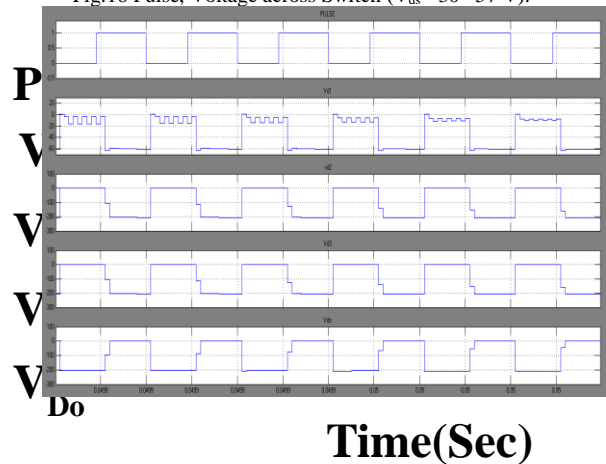


Fig.17 Pulse, Voltage across Diodes.($V_{D1}=60$ V, $V_{D2}=V_{D3}=V_{D0}=200$ V).

From fig.17, V_{D2} , V_{D3} , V_{D0} are equal and so, they are under the same voltage ratio, the voltage stresses can be adjusted by the turn ratio of the coupled inductor.

TABLE II
COMPARISON BETWEEN PROPOSED CONVERTER WITH PICONTROLLER & FLC

S.No	Type	Input Voltage (V)	Output Voltage (V)	Voltage Gain	Switch Voltage Stress (V)
1	Converter with PI controller	24	398.3	16.5	55-60
2	Converter with FLC	24	399.4	16.6	30-57

VIII.CONCLUSIONS

Here a high step-up dc–dc converter using coupled inductor with fuzzy logic control is simulated. By the capacitor charged in parallel and discharged in series by the coupled inductor, high step-up voltage gain is achieved. As the output voltage of the converter with FLC has minimum overshoot and produces a constant output current shows the better performance compared to the converter with PI controller. These studies could solve many types of problems regardless on stability because as we know that fuzzy logic controller is an intelligent controller to their appliances. Additionally, the switch voltage stress is reduced, thus a switch with low voltage ratings can be selected.

REFERENCES

- [1] Q. Zhao and F. C. Lee, “High-efficiency, high step-up dc–dc converters,” *IEEE Trans. Power Electron.*, vol. 18, no. 1, pp. 65–73, Jan. 2003.
- [2] T.F. Wu, Y.S. Lai, J.C. Hung and Y.M. Chen, “Boost Converter with Coupled Inductors and Buck–Boost Type of Active Clamp” *IEEE Trans Ind. Electron.*, vol. 55, no. 1, Jan. 2008.
- [3] B. Axelrod, Y. Berkovich and A.Ioinovici, “Switched Capacitor/Switched-Inductor Structures for Getting Transformerless Hybrid DC–DC PWM Converters”, *IEEE Trans Circuits And Systems—I: Regular Papers*, Vol. 55, no. 2, Mar 2008.
- [4] R.J. Wai, C.Y. Lin, C.Y. Lin, R.Y. Duan and Y.R. Chang, “High-Efficiency Power Conversion System for Kilowatt-Level Stand-Alone Generation Unit with Low Input Voltage”, *IEEE Trans Ind. Electron.*, vol. 55, no. 10, Oct 2008.
- [5] J.M. Kwon and B.W. Kwon, “High Step-Up Active-Clamp Converter with Input-Current Doubler and Output-Voltage Doubler for Fuel Cell Power Systems”, *IEEE Trans. Power Electron.*, vol. 24, no. 1, Jan 2009.
- [6] J. A. Carr, D. Hotz, J. C. Balda, A. Mantooth, A. Ong and A. Agarwal, “Assessing the Impact of SiC MOSFETs on Converter Interfaces for Distributed Energy Resources”, *IEEE Trans. Power Electron.*, vol. 24, no. 1, Jan 2009.
- [7] G.S. Yang, T.J. Liang and J.F. Chen, “Transformerless DC–DC Converters With High Step-Up Voltage”, *IEEE Trans Ind. Electron.*, vol. 56, no. 8, Aug 2009.
- [8] S.V. Araújo, R.P.T. Bascopé and G.V.T. Bascopé, “Highly Efficient High Step-Up Converter for Fuel-Cell Power Processing Based on Three-State Commutation Cell”, *IEEE Trans Ind. Electron.*, vol. 57, no. 6, June 2010.
- [9] S.K. Changchien, T.J Liang, J.F. Chen and L.S. Yang, “Novel High Step-Up DC–DC Converter for Fuel Cell Energy Conversion System”, *IEEE Trans Ind. Electron.*, vol. 57, no. 6, June 2010.
- [10] Y. Zhao, Y. Deng and Xiangning, “Interleaved Converter with Voltage Multiplier Cell for High Step-Up and High-Efficiency Conversion”, *IEEE Trans. Power Electron.*, vol. 25, no. 9, Sep 2010.
- [11] J. Bauman and M. Kazerani, “A Novel Capacitor-Switched Regenerative Snubber for DC/DC Boost Converters”, *IEEE Trans Ind. Electron.*, vol. 58, no. 2, Feb 2011.
- [12] Y.P. Hsieh, J.F. Chen, T.J Liang and L.S. Yang, “Novel High Step-Up DC–DC Converter with Coupled-Inductor and Switched-Capacitor Techniques for a Sustainable Energy System”, *IEEE Trans. Power Electron.*, vol. 26, no. 12, Dec 2011.
- [13] J.H. Lee, J.H. Park and J. H. Jeon, “Series-Connected Forward–Flyback Converter for High Step-Up Power Conversion”, *IEEE Trans. Power Electron.*, vol. 26, no. 12, Dec 2011.
- [14] Wuhua Li, Weichen Li, Xiangning He, David Xu and Bin Wu, “General Derivation Law of Nonisolated High-Step-Up Interleaved Converters with Built-In Transformer”, *IEEE Trans Industrial Electron.*, Vol. 59, no. 3, Mar 2012.
- [15] T.J. Liang, S.M. Chen, L.S. Yang, J.F. Chen, and A. Ioinovici, “Ultra-Large Gain Step-Up Switched-Capacitor DC-DC Converter With Coupled Inductor for Alternative Sources of Energy”, *IEEE Trans Circuits And Systems—I: Regular Papers*, vol. 59, no. 4, Apr 2012.
- [16] F.L. Tofoli, D.S. Oliveira, Jr., Ren’e Pastor Torrico-Bascop’e, and Y.J.C. Alcazar, “Novel Nonisolated High-Voltage Gain DC–DC Converters Based on 3SSC and VCM”, *IEEE Trans. Power Electron.*, vol. 27, no. 9, Sep 2012.
- [17] J.M. Burkhart, R. Korsunsky, and D.J. Perreault, “Design Methodology For A Very High Frequency Resonant Boost Converter”, *IEEE Trans. Power Electron.*, vol. 28, no. 4, Apr 2013.
- [18] F.S. Garcia, J.A. Pomilio and G. Spiazzi, “Modeling and Control Design of the Interleaved Double Dual Boost Converter”, *IEEE Trans Ind. Electron.*, vol. 60, no. 8, Aug 2013.
- [19] F.H. Dupont, C. Rech, R. Gules and J. R. Pinheiro, “Reduced-Order Model and Control Approach for the Boost Converter With a Voltage Multiplier Cell”, *IEEE Trans Power Electron.*, vol. 28, no. 7, July 2013.
- [20] R. J. Wai and R. Y. Duan, “High step-up converter with coupled inductor,” *IEEE Trans. Power Electron.*, vol. 20, no. 5, pp. 1025–1035, Sep. 2005.
- [21] R. J. Wai, L. W. Liu and R. Y. Duan, “High-efficiency voltage-clamped dc–dc converter with reduced reverse-recovery current and switch voltage stress,” *IEEE Trans. Ind. Electron.*, vol. 53, no. 1, pp. 272–280, Feb. 2005.
- [22] J. W. Baek, M. H. Ryoo, T. J. Kim, D. W. Yoo and J. S. Kim, “High boost converter using voltage multiplier,” in *Proc. IEEE IECON*, 2005, pp. 567–572.